



Cite this: DOI: 10.1039/c8nj04255a

An I₆P₇ peptide modified fluorescent probe for bio-imaging†

 Yuxin Yao,^{‡a} Lijuan Gui,^{‡a} Beike Gao,^b Zhenwei Yuan,^a Yisha Chen,^a Chen Wei,^a Qing He,^a Fei Wang,^a Mingjun Xu ^a and Haiyan Chen ^{*a}

The I₆P₇ peptide was proved to specifically bind to the interleukin-6 receptor, which can be exploited as an effective tumor-targeting moiety. Herein, a novel tumor-targeting fluorescent probe (**DMP**) conjugated with the I₆P₇ peptide was designed and synthesized. This probe was validated to possess valuable photophysical properties. The biocompatibility was evaluated by investigating its cytotoxicity on HUVEC and U87 cells, respectively. The tumor cell affinity has been confirmed by bio-imaging of this probe on different human cancer cells (U87, A549 and MCF-7 cells) and normal cells (HUVEC cell). The probe demonstrates low cytotoxicity, high tumor cell affinity and favorable mitochondria-targeting capability. Overall, these results revealed that **DMP** can serve as an important fluorescent probe for tumor-targeted bio-imaging.

Received 20th August 2018,
Accepted 3rd December 2018

DOI: 10.1039/c8nj04255a

rsc.li/njc

Introduction

In recent years, biomarkers have been widely applied in clinics for cancer diagnosis. Interleukin-6 (IL-6) is a multifunctional cytokine characterized as a regulator of inflammatory and immune responses.¹ Nevertheless, the dysregulation of IL-6 and its receptor interleukin receptor (IL-6R) in human cancers has been validated by recent research studies.² IL-6R, a membrane-bound glycoprotein, has been detected to be overexpressed in several cancer cells, such as human glioma U87 cells, adenocarcinomic human alveolar basal epithelial A549 cells and cervical cancer cells.^{3–5} The identification of novel carcinoma biomarkers with higher specificity and sensitivity is eagerly demanded for cancer diagnosis and therapy. IL-6R is composed of a ligand-binding part, which is an 80 kDa molecule related directly to IL-6, and a signal-transduction component. This component is an IL-6Rβ chain, glycoprotein 130 (gp 130), whose function is to form binding sites of IL-6 with high affinity and to transduce signals.^{6,7} Many cellular functions (*e.g.* angiogenesis, cell mobility and differentiation) are affected by the mediation of IL-6 signaling *via* gp 130, which are greatly involved in the pathogenesis of several human cancers.^{8,9} Recently, a heptapeptide I₆P₇ (N to C terminus: LSLITRL) has been designed and synthesized to inhibit the binding between IL-6 and

IL-6R, ascribed to its high-efficiency of binding to IL-6R.³ Based on this, I₆P₇ could be modified as a potential tumor-targeting ligand for bio-imaging *in vitro* and *in vivo*.¹⁰

Optical imaging has emerged as an effective tool for bio-imaging due to its high spatial resolution, sensitivity, specificity and low-cost.^{11,12} The major problem, limited tissue penetration, could be resolved through designing near-infrared (NIR) fluorophores, under which tissues do not exhibit auto-fluorescence. Thus, NIR optical imaging is fitting for bio-imaging applications *in vivo*.^{13,14} In recent years, many fluorophores, which possess strong NIR absorption and emission properties, have been reported in the literature and applied in bio-imaging, including cyanine dye, coumarin, rhodamine, squaraine, BODIPY and dicyanomethylene-4*H*-pyran (DCM).^{15–20} In 2015, Tian *et al.* synthesized a diethylaminophenyl substituted BODIPY-based pH-activatable theranostic nanosystem.²¹ In addition, Choi's group utilized a NIR fluorescent probe to realize tissue-specific imaging.²² Compared with others, DCM was capable of exhibiting better photo-stability, which was more suitable for application in biological samples.^{16,23–26} However, DCM-type derivatives have seldom been developed for tumor-targeting.

With this goal in mind, a novel DCM derivative fluorescent probe (**DMP**) decorated with I₆P₇ for bio-imaging was designed and synthesized. It exhibited a strong absorption band at 420 nm and an emission peak at 705 nm. **DMP** showed good biocompatibility in tumor cells and good solubility in water. The I₆P₇ peptide acts as a tumor targeting ligand, increasing the ability of the probe to specifically target tumor cells. Moreover, the targeting ability was validated using multiple cell lines. The results revealed the feasibility of **DMP** for targeting IL-6R and promising application in bio-imaging.

^a Department of Biomedical Engineering, School of Engineering, China Pharmaceutical University, 24 Tongjia Lane, Gulou District, Nanjing, 210009, China. E-mail: chenhaiyan@cpu.edu.cn

^b Jiangsu XinHai Senior High School, No. 58 Cangwu Road, Haizhou District, Lianyungang, 222006, China. E-mail: 2532267562@qq.com

† Electronic supplementary information (ESI) available. See DOI: 10.1039/c8nj04255a

‡ These authors contributed equally to this work.

Results and discussion

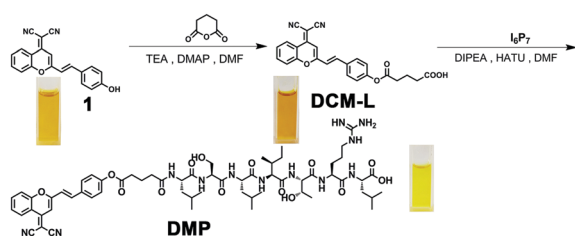
Design and synthesis of DMP

A novel NIR fluorescent probe capable of bio-imaging was designed and synthesized (Scheme 1). **DMP** consists of a fluorescence reporting group (a DCM dye) and a tumor-targeting group (I_6P_7). The fluorescence reporting group was conjugated with I_6P_7 through monomethyl esterification with glutaric anhydride with a satisfactory yield of 19.76%. All the structures of the compounds concerned above were validated by 1H NMR and MALDI-TOF-MS (Fig. S2–S7, ESI $^+$).

Optical response of I_6P_7 to DCM-L

A spectroscopic experiment was performed in PBS buffer (pH = 7.4, 10 mM) with 50% DMSO (compound **1** and **DCM-L**) or 10% DMSO (**DMP**) at 37 °C. As shown in Fig. 1, the absorption and fluorescence spectra of compound **1**, **DCM-L** and **DMP** were investigated. The absorbance spectra of compound **1** and **DCM-L** show an absorption band from 500 nm to 600 nm with an absorption peak at 555 nm (Fig. 1A). The fluorescence spectra were extended to a wide range from 600 nm to 850 nm with a peak at 705 nm (Fig. 1B). And **DMP** exhibited a new absorption at 420 nm and two fluorescence peaks extending from 650 to 720 nm. Compared with **1** and **DCM-L**, **DMP** exhibits a larger Stokes shift, which can improve detection sensitivity. Furthermore, the difference of dissolution systems between **DMP** (10% DMSO) and **1** and **DCM-L** (50% DMSO) demonstrated that **DMP** had better solubility in the aqueous phase. The changes could be due to the I_6P_7 peptide.

The stability of probe **DMP** at different pH values and in different solutions was further investigated (Fig. 2). As indicated in Fig. 2A, the absorbance spectra and fluorescence spectra display a weak change at pH values ranging from 4 to 8. At a higher pH value, the intensity decreases. Based on the above results,



Scheme 1 Synthesis of probe **DMP**.

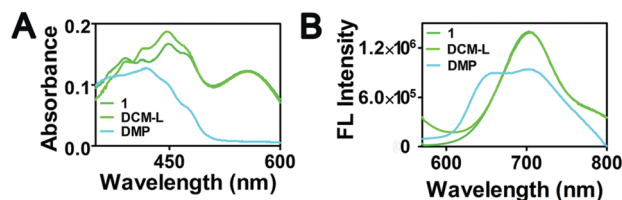


Fig. 1 Absorbance (A) and fluorescence (B) spectra of compound **1** (10 μ M) and **DCM-L** (10 μ M) in a DMSO/PBS solution (50/50, v/v, pH 7.4, 10 mM) and **DMP** (10 μ M) in PBS buffer (pH = 7.4) containing 10% DMSO. λ_{ex} (**1**, **DCM-L**) = 555 nm; and λ_{ex} (**DMP**) = 420 nm.

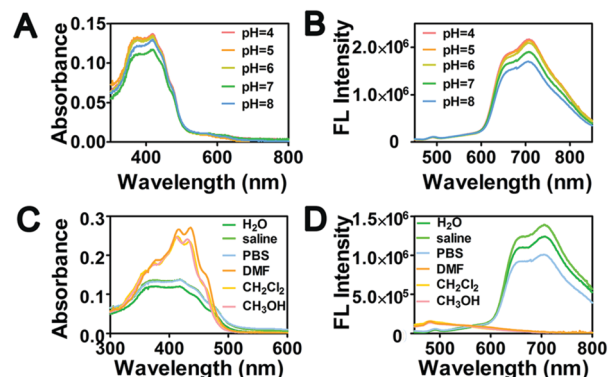


Fig. 2 (A) Absorbance and (B) fluorescence spectra of compound **DMP** (10 μ M) in PBS buffer with different pHs (pH = 4, 5, 6, 7, 8) and saline containing 1% DMSO. (C) Absorbance and (D) fluorescence spectra of compound **DMP** (10 μ M) in different solutions (H_2O , saline, PBS, CH_2Cl_2 , CH_3OH , DMF) containing 1% DMSO. λ_{ex} = 420 nm.

DMP is steady at pH values ranging from 4 to 8. The absorbance and fluorescence spectra of **DMP** in different solutions further illustrated that it can present better photophysical properties in inorganic solutions, which supported the conclusion above.

Cytotoxicity assay

In order to evaluate the cell affinity of **DMP**, the biocompatibility was investigated on HUVEC cells and U87 cells firstly. The cytotoxicity of **DMP** was evaluated using conventional MTT assays (Fig. 3 and Fig. S8, ESI $^+$). As shown in Fig. 3A, even after being treated with a relatively high concentration of the probes (80 μ M) for 72 h, the viability of the HUVEC cells was still maintained above 95%, which means that the probe did not show any conspicuous cytotoxicity and had good biocompatibility. Excitingly, Fig. 3B illustrates that when **DCM-L** was conjugated with the I_6P_7 peptide, the viability of U87 cells incubated with **DMP** for 72 h began to display a downward trend.

Cell affinity evaluation of **DMP**

For efficient tumor targeting of the NIR probes, compound **DCM-L** was conjugated to the I_6P_7 peptide to target IL-6R. The I_6P_7 sequence has high affinity for IL-6R, which is over-expressed in many tumor cells. The schematic diagram of tumor cell imaged by the probe **DMP** was shown in Scheme 2. The cell affinity of **DMP** was further investigated on IL-6R over-expressed cells (A549, MCF-7 and U87) using confocal fluorescence microscopy.^{27–29} As shown in Fig. 4, the green channel enabled

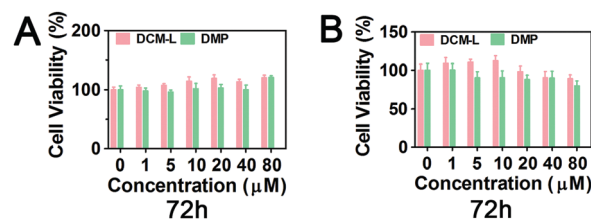
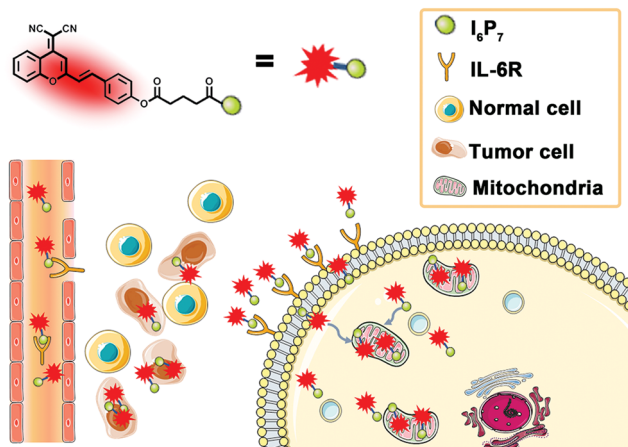


Fig. 3 Cell viability of HUVEC (A) and U87 (B) cells incubated with **DCM-L** and **DMP** for 72 h, respectively. Data are expressed as mean \pm S.D. (n = 4).



Scheme 2 The schematic diagram of tumor cell imaged by the probe **DMP**.

DMP showed a gradual increase with increasing time. The fluorescence is strongest at 2 h after incubation with **DMP** (Fig. 4A). To validate the tumor targeting ability of **DMP** in other tumor cells, the confocal fluorescence imaging of U87 cells and MCF-7 cells was further performed. Similar results can be observed on U87 and MCF-7 cells, as shown in Fig. 4D and G. The semi-quantitative analysis of the fluorescence intensity at three different time periods (0.5 h, 1 h and 2 h) manifests a more intuitive presentation (Fig. 4B, E and H). Furthermore, colocalization experiments were performed by co-staining the tumor cells to evaluate the subcellular localization. The punctate distribution of fluorescence is consistent with fluorescence activation occurring in the mitochondria. When the fluorescence signal from **DMP** (red) showed substantial overlap with the mitochondria stain (green), the resulting image is yellow or orange. The fluorescent signal of the linear regions of interest (ROI) showed a tendency to synchronize with a

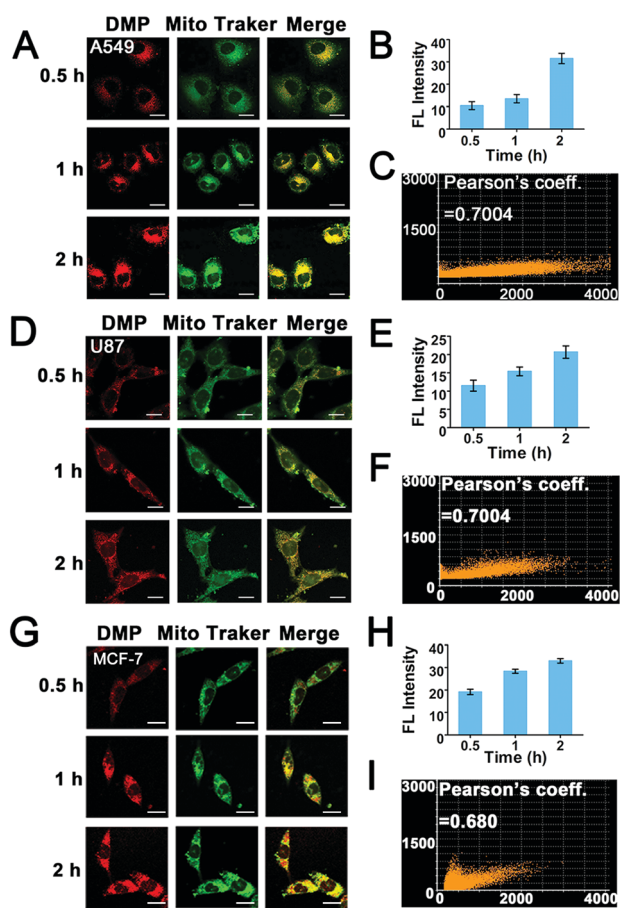


Fig. 4 LCFM fluorescence images of **DMP** in A549, U87 and MCF-7 cells. (A, D, and G) Fluorescence imaging of A549, U87 and MCF-7 cells stained with **DMP** (80 μM , $\lambda_{\text{ex}} = 405 \text{ nm}$). The cells were incubated with **DMP** at 37 $^{\circ}\text{C}$ for 0.5 h, 1 h and 2 h. (B, E, and H) Semi-quantitative fluorescence intensity analysis. (C, F, and I) Linear profile and scatter plot were used to characterize the overlap degree of red fluorescence from **DMP** and green fluorescence from MitoTracker Green. Scale bar: 20 μm .

visualization of the mitochondria using MitoTracker Green and the red channel enabled visualization using **DMP**. A time-dependent investigation was further carried out. The fluorescence intensity of

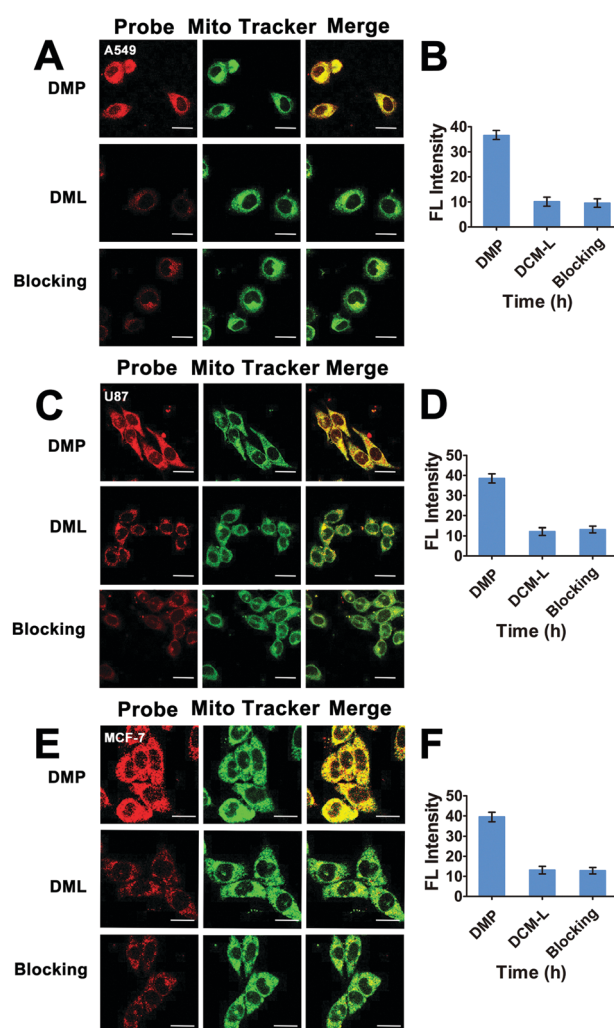


Fig. 5 LCFM fluorescence images of the probes in A549, U87 and MCF-7 cells. (A, C and E) Fluorescence imaging of A549, U87 and MCF-7 cells stained with **DMP** (80 μM , $\lambda_{\text{ex}} = 405 \text{ nm}$) and **DCM-L** (80 μM). The cells were incubated with **DMP** and **DCM-L** at 37 $^{\circ}\text{C}$ for 2 h. The blocking experiments were carried out by adding a free I_6P_7 peptide (80 μM) into the cells prior to **DMP** incubation. (B, D and F) Semi-quantitative fluorescence intensity analysis. Scale bar: 20 μm .

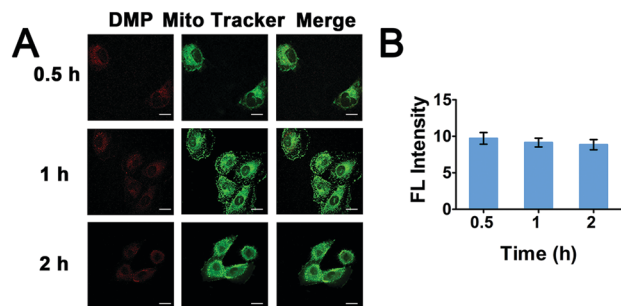


Fig. 6 LCFM fluorescence images of **DMP** in HUVEC cells. (A) Fluorescence imaging of HUVEC cells stained with **DMP** (100 μM , $\lambda_{\text{ex}} = 405 \text{ nm}$). The cells were incubated with **DMP** at 37 $^{\circ}\text{C}$ for 0.5 h, 1 h and 2 h. (B) Semi-quantitative fluorescent intensity analysis. Scale bar: 20 μm .

Pearson co-localization coefficient of 0.70 for A549 cells, 0.70 for U87 and 0.68 for MCF-7 cultivated with **DMP** (Fig. 4C, F and I). The results shown above indicate the capability of **DMP** to selectively target the mitochondria in tumor cells rather than other organelles.

To further verify the tumor cell affinity of the probe, different tumor cells were incubated with **DMP** and **DCM-L**. As shown in Fig. 5, the fluorescence images of A549, U87 and MCF-7 cells incubated with **DMP** and **DCM-L** for 2 hours were acquired. A549, U87, and MCF-7 cells incubated with **DMP** emitted strong fluorescence signals, compared with the **DCM-L** group, which indicated that the introduction of the I₆P₇ peptide increased the tumor cell affinity of **DMP**. Furthermore, when the free I₆P₇ peptide was added before incubation with **DMP**, the tumor cells exhibited slight fluorescence, which indicated that the free I₆P₇ peptide competed with **DMP** for binding IL-6R.

Furthermore, the fluorescence signals of **DMP** within the mitochondria were also investigated in HUVEC cells. The result depicted in Fig. 6 indicates that fairly weak fluorescence was observed in HUVEC cells after incubation with **DMP** for 2 hours. The semi-quantitative analysis also indicated that no distinct fluorescence enhancement appeared as the time extended (Fig. 6B). These results also verified the important role of the I₆P₇ peptide in terms of the tumor-targeting capability of the probe.

Conclusions

In summary, we have developed an effective fluorescent probe (**DMP**) with a targeted peptide. The probe shows low cytotoxicity and excellent photophysical properties. Moreover, the targeting ability is also verified in several kinds of cells. These experimental results show the feasibility of targeting IL-6R and its potential use as a small molecular probe in future. However, as IL-6/IL-6R exists in many diseases, the probe cannot target tumors exactly. An *in vivo* experiment should be carried out to verify the target ability in future.

Experimental

Reagents and instruments

1-(2-Hydroxyphenyl)ethanone, malononitrile and 4-hydroxybenzaldehyde were purchased from Shanghai Macklin Biochemical Co. Ltd (Shanghai, China). Peptide I₆P₇ was obtained

from Nanjing Peptide Co. Ltd (Jiangsu, China). Mito-Tracker Green was purchased from KeyGen BioTech (Jiangsu, China). 3-(4,5-Dimethylthiazol-2-yl)-2,5-diphenyltetrazolium bromide (MTT), Dulbecco's modified Eagle's medium (DMEM), fetal bovine serum (FBS), penicillin, streptomycin, and trypsin-EDTA were purchased from the Institute of Biochemistry and Cell Biology, SIBS, CAS (China). All other chemicals were supplied by J&K Scientific Ltd (Beijing, China) or Sinopharm chemical reagent Co. Ltd (Shanghai, China) and utilized without further purification. Ultrapure water from a Milli-Q reference system (Millipore) was utilized in all experiments. Silica gel (100–200 mesh) was used for silica column chromatography.

Nuclear magnetic resonance (NMR) spectra were recorded on a Bruker Avance III-300 instrument (Bruker, Billerica, MA, USA) at 500 MHz for ^1H NMR, and TMS was utilized as an internal reference. Mass spectra were collected on a tandem quadrupole mass spectrometer (Waters, Milford, MA, USA) with a MALDI-TOF-MS resource and an AB SCIEX 5800 matrix-assisted laser desorption ionization time-of-flight (MALDI-TOF) mass spectrometer (SCIEX, Beijing, China), respectively. Absorption spectra were recorded on a Lambda 25 UV-vis spectrophotometer (PerkinElmer, USA), and fluorescence spectra were obtained by using a PerkinElmer-LS55 spectrophotometer (PerkinElmer, USA).

Synthesis of **DMP** and **DCM-L**

Compound **1**, (*E*)-2-(2-(4-hydroxystyryl)-4H-chromen-4-ylidene) malononitrile, was synthesized according to the reported method.³⁰ The synthesis routine is shown in Fig. S1 (ESI[†]). Compounds **DCM-L** and **DMP** were fabricated by the following method (Scheme 1). Compound **DCM-L**: compound **1** (800.00 mg, 2.56 mmol, 1 equiv.) was dissolved in 10 mL anhydrous *N,N*-dimethylformamide (DMF). Then dihydro-2H-pyran-2,6 (3*H*)-dione (1.46 g, 12.81 mmol, 5 equiv.) and *N,N*-dimethylpyridin-4-amine (DMAP) (625.86 mg, 5.12 mmol, 2 equiv.) were added followed by dropwise addition of triethylamine (TEA) (1.30 g, 12.81 mmol, 5 equiv.) under nitrogen protection at room temperature. The resulting mixture was stirred overnight. The solvent was removed under vacuum and further purified by silica gel column chromatography to afford the compound **DCM-L** as a yellow solid: yield 352 mg, 44%. ^1H NMR (500 MHz, DMSO-*d*₆) δ 12.09 (s, 1H), 8.75 (s, 1H), 7.93 (d, *J* = 10 Hz, 1H), 7.89–7.72 (m, 3H), 7.65 (m, 3H), 7.28 (d, *J* = 16 Hz, 1H), 6.97 (d, *J* = 16 Hz, 1H), 6.88 (d, *J* = 5 Hz, 1H), 2.73 (t, *J* = 5 Hz, 2H), 2.41–2.32 (m, 2H), 1.94–1.85 (m, 2H). ^{13}C NMR (125 MHz, DMSO-*d*₆) δ (ppm): 174.45, 171.75, 158.38, 153.32, 152.44, 152.32, 138.00, 135.92, 133.10, 129.82, 126.65, 125.11, 123.00, 120.22, 119.52, 117.52, 116.20, 107.31, 61.01, 33.24, 33.08, 20.28. MALDI-TOF-MS calculated for C₂₅H₁₈N₂O₅: 426.43, found 425.0754.

Compound **DMP**. Compound **DCM-L** (100.00 mg, 234.51 μmol , 1 equiv.) and 1-[bis(dimethylamino)methylene]-1*H*-1,2,3-triazolo [4,5-*b*]pyridinium 3-oxide hexafluorophosphate (HATU) (183.05 mg, 351.77 μmol , 1.5 equiv.) were dissolved in 5 mL DMF with *N*-ethyl-diisopropylamine (DIPEA) (45.46 mg, 351.77 μmol , 1.5 equiv.). The peptide I₆P₇ was added after the mixture was stirred at room temperature for 10 min. The resulting mixture was stirred at room temperature for 30 min. Then the reaction

mixture was recrystallized with diethyl ether three times to generate compound **DMP**: yield 56.70 mg, 19.76%. ^1H NMR (500 MHz, DMSO- d_6) δ 12.80 (s, 1H), 8.76 (s, 1H), 8.67 (s, 1H), 8.45 (s, 1H), 8.13 (s, 2H), 8.03 (s, 1H), 7.97–7.92 (m, 1H), 7.87–7.77 (m, 4H), 7.64 (d, J = 7.5 Hz, 1H), 7.58–7.40 (m, 3H), 7.27 (d, J = 15 Hz, 2H), 7.06 (d, J = 16 Hz, 1H), 6.76 (s, 2H), 4.99 (s, 1H), 4.43–4.14 (m, 7H), 3.96 (s, 1H), 3.59 (m, 4H), 3.09 (m, 2H), 2.71 (d, J = 25 Hz, 2H), 2.61 (m, 1H), 2.51 (s, 1H), 2.28 (s, 2H), 1.88 (m, 2H), 1.80–1.32 (m, 15H), 1.27–1.01 (m, 6H), 0.95–0.62 (m, 21H). ^{13}C NMR (125 MHz, DMSO- d_6) δ 174.30, 173.02, 172.36, 172.33, 171.78, 171.51, 170.45, 169.92, 162.7, 158.44, 157.13, 153.44, 152.51, 152.35, 138.05, 135.97, 133.12, 130.83, 129.82, 126.70, 123.03, 120.27, 119.56, 117.58, 116.53, 116.38, 116.24, 107.35, 106.17, 67.02, 61.89, 61.01, 58.49, 57.49, 55.58, 53.97, 52.29, 51.76, 50.80, 42.25, 41.13, 40.98, 38.72, 36.71, 36.26, 34.43, 33.36, 31.26, 25.24, 24.70, 24.57, 23.58, 23.51, 23.33, 21.96, 21.74, 19.71, 15.81, 11.44. MALDI-TOF-MS calculated for $\text{C}_{62}\text{H}_{86}\text{N}_{12}\text{O}_{14}$: 1222.64, found 1223.6.

In vitro characterization

UV-vis and fluorescence measurements of compound **1** and **DCM-L** were carried out in a PBS solution containing 50% dimethyl sulfoxide (DMSO), pH 7.4. Fluorescence spectra were recorded in the range of 500 to 800 nm under irradiation with a laser. Stock solutions of **1**, **DCM-L** and **DMP** (1 mM) in DMSO were initially prepared. In a 3.0 mL tube, PBS buffer (10 mM, pH 7.4, 2 mL) and the above stock solutions were mixed. The final solution volume was adjusted to 3.0 mL with PBS buffer. After rapid mixing of the solution, it was transferred to a 10×10 mm quartz cell and incubated at 37 °C for *in vitro* detection.

Cell culture

A549 cells (adenocarcinomic human alveolar basal epithelial cells), MCF-7 cells (human breast adenocarcinoma cells), U87 cell (human glioma cells) and HUVEC cells (human umbilical vein endothelial cells) were obtained from American Type Culture Collection (ATCC, USA). The cell lines were cultivated on glass-bottom culture dishes in an atmosphere of 5% CO_2 at 37 °C in DMEM supplemented with 10% FBS and 1% (v/v) penicillin–streptomycin.

Cytotoxicity assay

The *in vitro* cytotoxicity of the probe to HUVEC and U87 cell lines was measured by MTT assay. Briefly, the cells were loaded in 96-well culture plates at 7000 cells per well and subsequently incubated for 24 h in a CO_2 culture box. After culture for 24 h, the cells were further maintained at 37 °C for 24 h under 5% CO_2 after treatment of probes **DCM-L** and **DMP** (100 μL per well) at a wide concentration range from 0 to 80 μM . Then to each well was added MTT (20 μL , 5.0 mg mL^{-1}) and the cells were incubated for another 4 h. The medium containing MTT was then carefully removed and 150 μL of DMSO was added into each well. The plates were gently shaken for 15 min at room temperature before the absorbance measurements. The absorbance at 490 nm was measured in a 96-well microplate reader. Seven independent experiments were carried out for *in vitro*

cytotoxicity analysis. The following formula was used to calculate the viability of cell growth: viability (%) = (mean absorbance of the test wells – mean absorbance of the medium control wells)/(mean absorbance of the untreated wells – mean absorbance of the medium control wells) \times 100%.

Fluorescence imaging cell analysis using the probes

A549, MCF-7 and U87 cells, which are known to overexpress IL-6R under hypoxic conditions, are selected to assess the applicability of **DMP** in intracellular IL-6R monitoring. The cells were seeded in laser scanning confocal microscope (LSCM) culture dishes at a density of 5×10^5 cells per well and subsequently incubated at 37 °C in a humidified atmosphere containing 5% CO_2 . When the whole cells took up 70–80% space of the culture dishes, the cells were treated with **DMP** (100 μM) in DMSO/PBS buffer (1 : 99, v/v) for 30 min, 60 min and 90 min, respectively. For mitochondrial staining, the cells were stained with Mito-Tracker Green (1.0 μM) for 30 min and then washed with PBS buffer three times to remove the free dye. Blocking experiments were carried out, in which the cells were incubated with free I_6P_7 peptide for 0.5 h prior to incubation with **DMP**. Fluorescence images were recorded on an FV1000 confocal fluorescence microscope (Olympus, Japan). The fluorescence signal was collected at the NIR fluorescence channel (680 ± 30 nm, $\lambda_{\text{ex}} = 420$ nm), and green fluorescence channel (516 ± 30 nm, $\lambda_{\text{ex}} = 490$ nm), respectively.

Conflicts of interest

There are no conflicts to declare.

Acknowledgements

The authors are grateful to the Natural Science Foundation Committee of China (NSFC 81671803), the National Key Research and Development Program (Grant No. 2017YFC0107700), the Outstanding Youth Foundation of Jiangsu Province (GX20171114003, BK20170030), the Fok Ying Tung Education Foundation (161033), the “Double First-Class” University project (CPU2018GY06) and the Priority Academic Program Development of Jiangsu Higher Education Institutions for their financial support.

Notes and references

- 1 R. Malhotra, V. Patel, J. P. Vaqu e, J. S. Gutkind and J. F. Rusling, *Anal. Chem.*, 2010, **82**, 3118–3123.
- 2 D. S. Hong, L. S. Angelo and R. Kurzrock, *Cancer*, 2007, **110**, 1911–1928.
- 3 J. L. Su, K. P. Lai, C. A. Chen, C. Y. Yang, P. S. Chen, C. C. Chang, C. H. Chou, C. L. Hu, M. L. Kuo and C. Y. Hsieh, *Cancer Res.*, 2005, **65**, 4827.
- 4 W. Pan, C. Yu, H. Hsuchou, Y. Zhang and A. J. Kastin, *Am. J. Physiol.: Cell Physiol.*, 2008, **294**, 1436–1442.
- 5 A. Sturzu and S. Heckl, *Chem. Biol. Drug Des.*, 2010, **75**, 369–374.

- 6 T. Kishimoto and T. Taga, *Science*, 1992, **258**, 593–597.
- 7 M. Hibi, M. Murakami, M. Saito, T. Hirano, T. Taga and T. Kishimoto, *Cell*, 1990, **63**, 1149–1157.
- 8 B. Dankbar, T. Padró, R. Leo, B. Feldmann, M. Kropff, R. M. Mesters, H. Serve, W. E. Berdel and J. Kienast, *Blood*, 2000, **95**, 2630–2636.
- 9 S. H. Jee, C. Y. Chu, H. C. Chiu, Y. L. Huang, W. L. Tsai, Y. H. Liao and M. L. Kuo, *J. Invest. Dermatol.*, 2004, **123**, 1169–1175.
- 10 S. Wang, S. Reinhard, C. Li, M. Qian, H. Jiang, Y. Du, U. Lachelt, W. Lu, E. Wagner and R. Huang, *Mol. Ther.*, 2017, **25**, 1556–1566.
- 11 P. Nalbant, L. Hodgson, V. Kraynov, A. Toutchkine and K. M. Hahn, *Science*, 2004, **305**, 1615–1619.
- 12 K. Hanaoka, K. Kikuchi, S. Kobayashi and T. Nagano, *J. Am. Chem. Soc.*, 2007, **129**, 13502–15309.
- 13 B. Ballou, L. A. Ernst and A. S. Waggoner, *Curr. Med. Chem.*, 2005, **12**, 795–805.
- 14 J. Rao, A. Dragulescu-Andrasi and H. Yao, *Curr. Opin. Biotechnol.*, 2007, **18**, 17–25.
- 15 J. Cao, C. Zhao, X. Wang, Y. Zhang and W. Zhu, *Chem. Commun.*, 2012, **48**, 9897–9899.
- 16 K. Gu, Y. Xu, H. Li, Z. Guo, S. Zhu, S. Zhu, P. Shi, T. D. James, H. Tian and W. H. Zhu, *J. Am. Chem. Soc.*, 2016, **138**, 5334–5340.
- 17 M. Gao, F. Yu, C. Lv, J. Choo and L. Chen, *Chem. Soc. Rev.*, 2017, **46**, 2237–2271.
- 18 Z. Xue, H. Zhao, J. Liu, J. Han and S. Han, *Chem. Sci.*, 2017, **8**, 1915–1921.
- 19 T. Myochin, K. Hanaoka, S. Iwaki, T. Ueno, T. Komatsu, T. Terai, T. Nagano and Y. Urano, *J. Am. Chem. Soc.*, 2015, **137**, 4759–4765.
- 20 M. Ye, X. Wang, J. Tang, Z. Guo, Y. Shen, H. Tian and W. H. Zhu, *Chem. Sci.*, 2016, **7**, 4958–4965.
- 21 J. Tian, J. Zhou, S. Zhen, D. Lin, J. S. Yu and H. Ju, *Chem. Sci.*, 2015, **6**, 5969–5977.
- 22 E. A. Owens, M. Henary, G. El Fakhri and H. S. Choi, *Acc. Chem. Res.*, 2016, **49**, 1731–1740.
- 23 M. Li, X. Wu, Y. Wang, Y. Li, W. Zhu and T. D. James, *Chem. Commun.*, 2014, **50**, 1751–1753.
- 24 O. Green, S. Gnaim, R. Blau, A. Eldar-Boock, R. Satchi-Fainaro and D. Shabat, *J. Am. Chem. Soc.*, 2017, **139**, 13243–13248.
- 25 X. Wu, X. Sun, Z. Guo, J. Tang, Y. Shen, T. D. James, H. Tian and W. Zhu, *J. Am. Chem. Soc.*, 2014, **136**, 3579–3588.
- 26 W. Sun, J. Fan, C. Hu, J. Cao, H. Zhang, X. Xiong, J. Wang, S. Cui, S. Sun and X. Peng, *Chem. Commun.*, 2013, **49**, 3890–3892.
- 27 M. Bihl, M. Tamm, M. Nauck, H. Wieland, A. P. Perruchoud and M. Roth, *Am. J. Respir. Cell Mol. Biol.*, 1998, **19**, 606–612.
- 28 A. Tchirkov, C. Rolhion, S. Bertrand, J. F. Dore, J. J. Dubost and P. Verrelle, *Br. J. Cancer*, 2001, **85**, 518–522.
- 29 N. J. Sullivan, A. K. Sasser, A. E. Axel, F. Vesuna, V. Raman, N. Ramirez, T. M. Oberyzyzn and B. M. Hall, *Oncogene*, 2009, **28**, 2940–2947.
- 30 J. Wang, B. Li, W. Zhao, X. Zhang, X. Luo, M. E. Corkins, S. L. Cole, C. Wang, Y. Xiao, X. Bi, Y. Pang, C. A. McElroy, A. J. Bird and Y. Dong, *ACS Sens.*, 2016, **1**, 882–887.